Volume 7, Issue 1, 2017, 1921 - 1926 ISSN 2069-5837

Biointerface Research in Applied Chemistry

www.BiointerfaceResearch.com

Original Research Article Open Access Journal

Received: 07.01.2017 / Revised: 30.01.2017 / Accepted: 10.02.2017 / Published on-line: 15.02.2017

Ultrasensitive detection of neurotransmitters by surface enhanced raman spectroscopy for biosensing applications

Chao Qiu [1], Kevin E. Bennet [2, 3], Jonathan R. Tomshine [2], Seth Hara [2], John D. Ciubuc [1], Ute Schmidt [4], William G. Durrer [1], Malcolm B. McIntosh [3], Michael Eastman [5], Felicia S. Manciu [1, 6, *]

[1] Department of Physics, University of Texas at El Paso, El Paso, TX 79968, USA
[2] Department of Neurologic Surgery, Mayo Clinic, Rochester, MN 55905, USA
[3] Division of Engineering, Mayo Clinic, Rochester, MN 55905, USA
[4] WITec GmbH, Ulm 89081, Germany
[5] Department of Chemistry, University of Texas at El Paso, El Paso, TX 79968, USA
[6] Border Biomedical Research Center, University of Texas at El Paso, El Paso, TX 79968, USA

*corresponding author e-mail address: ***fsmanciu@utep.edu***

ABSTRACT

Detection of trace amounts of neurotransmitters has become significant in diagnostic applications. A powerful analytical tool, surface-enhanced Raman spectroscopy (SERS) has been used to detect serotonin, adenosine, and dopamine. In this study, silver nanoparticles (Ag NPs) were utilized as SERS-active substrates for high sensitivity detection of these analytes, in very low sub-nanomolar concentrations. The high resolution, real-time Raman spectra were recorded in about 500 milliseconds. Since at the molecular level, neurotransmitters can be present in the proximity of metallic nanoparticles in different orientations or even adsorbed on them, inhomogeneous Raman enhancement is commonly observed, with SERS vibrational lines varying in their intensities and positions depending on the dominant orientation or on the underlining physico-chemical process. These variations might also be related to the intrinsic small Raman cross section of the molecules and to their concentration in the vicinity of Ag NPs. Thus, this SERS study, besides advancing knowledge of high sensitivity detection, also addresses possible adsorption effects.

Keywords: *surface-enhanced Raman spectroscopy, neurotransmitters, serotonin, adenosine, dopamine, silver nanoparticles, biosensing.*

1. INTRODUCTION

Since its discovery in the 1970s [1,2], surface-enhanced Raman scattering (SERS) has attracted significant attention, with a wide variety of uses, ranging from ultrasensitive chemical [3–5] and biomolecular sensing [6–10] to environmental analysis [11,12] and homeland security applications [13]. It is its unique ultrasensitivity in identifying molecular structures that makes SERS such a powerful analytical tool in so many research areas. Substantial advances have been achieved in the past two decades in developing new strategies for designing high-performance, sensitive, and reproducible SERS substrates [3–18]. Consequently, reliable materials have been fabricated, ranging from noble metals [3,6,10,12] to semiconductors [19] to hybrid composite materials [7,14,16,17]. However, for medical purposes, most of the SERS active substrates still rely on noble metal nanostructures and their derivatives [3,6–8,10].

Intrinsic surface plasmon resonance (SPR) at noble metal surfaces can greatly increase local electromagnetic fields [20]. With small and irregular surfaces, nanoscale structures can provide large numbers of Raman "hot spots," which have a synergistic effect on the magnification of the Raman signal. The sizes and shapes of nanoparticles are known to be critical for the overall SERS capabilities [5,21,22]. Thus, controlling and tuning these factors are of significant importance in SERS substrate design. Rigorous studies have been made, both experimentally and theoretically, for better understanding the properties of the relevant materials and for continuous improvement of the current variety of SERS substrates [3–22].

Serotonin, adenosine, and dopamine are very important neurotransmitters in the human central nervous system, as many neurological diseases are caused by lack or excess of them [23–25]. They have therefore been among the most studied of neurotransmitters [6,7,9,10,23–25]. Accurate determinations of their concentrations in biological systems are essential for disease monitoring. Although being able to detect and identify trace quantities of bioanalytes has become increasingly important in virtually every related scientific discipline and a variety of methods have been employed for neurotransmitter measurements such as amperometry [26], chromatography [27], fluorescence [28–34], and magnetic resonance spectroscopy (MRS) [35], their disadvantages regarding potential clinical use include detection times that are long compared to characteristic physiological processes and lack of capacity for reliable simultaneous detection of different neurotransmitters. As a result, considerable attention has been directed to developing new, sensitive detection methods that will improve selectivity as well as neurotransmitter detection limits. The technique most employed for such detection is based on voltammetry, with the current state-of-the art being fast scan cyclic voltammetry (FSCV) [36,37]. However, as demonstrated in this work, SERS can provide even higher sensitivity and selectivity in the detection of analytes than FSCV.

There are several challenges in using SERS to accurately identify neurotransmitters. These challenges include weak analyte affinity, oxidation of neurotransmitters, and stability of SERS substrates. As the analyte under study may be either physisorpted or chemisorpted onto the substrate, it is worth pointing out that the interaction range between the analyte and the substrate strongly influences the strength of any measurable SERS signal [8,22]. Furthermore, at the molecular level, neurotransmitters in the

proximity of the SERS substrate can be present in different orientations. Consequently, inhomogeneous Raman enhancement can result, with SERS vibrational lines varying in their intensities depending on locally, dominant orientations and the aforementioned effects. Not only does the current SERS study demonstrate detection of neurotransmitters for concentrations as low as 10^{-11} M, but it also addresses selectivity resulting from different SERS enhancement processes.

2. EXPERIMENTAL SECTION

2.1. Materials and sample preparation. The synthesis of silver nanoparticles (Ag NPs) was performed as previously reported in the literature [38]. Silver nitrate ($AgNO_3$, >99%) and Sodium borohydride ($NaBH_4$, >99%) reagents were purchased from Sigma-Aldrich and citric acid trisodium salt dihydrate ($C_6H_5Na_3O_7{\cdot}2H_2O$, 99%) from ACROS. 20 mL of 1% (w/v) citrate solution and 75 mL of ultrapure water were poured into a round bottom flask and the mixture was heated to 80°C until stable. Then, 1.7 mL of 1% (w/v) $AgNO_3$ solution was added to the mixture, followed quickly by the addition of 2 mL of 0.1% (w/v) freshly prepared $NaBH_4$ solution. The reaction solution was kept at 80°C under vigorous stirring for 30 min and cooled to room temperature. Finally, the mixture was purified by washing/resuspension and centrifugation several times to remove the excess of organic and unreacted impurities.

Generally, for Ag NP thin film fabrication, the synthesized Ag NPs were mixed with serotonin, adenosine, and dopamine in concentrations ranging from 10^{-5} M to 10^{-11} M. The mixed solutions were each sonicated for 20 seconds, then drop-cast on clean cover slips, and vacuum dried. Not only did the vacuum drying process help in avoiding unwanted neurotransmitter oxidation, but it also promoted the formation of dense and uniform Ag NP thin films. The films were stored under vacuum until characterization.

2.2. Experimental set-up and data acquisition. Scanning electron microscopy (SEM) images were acquired with a Hitachi S4700 SEM (Hitachi Ltd., Tokyo, Japan), with accelerating voltage and emission set to 5 kV and 8 μA, respectively. An *alpha 300RA WITec* modular system (WITec Inc., Ulm, Germany) that combines both confocal Raman and atomic force microscopy (AFM) was used for the corresponding investigations, which were performed in ambient conditions at room temperature. The surface topography of 4 × 4 μm^2 and 1 × 1 μm^2 areas on the films was measured in AFM AC mode. *Arrow Force Modulation* cantilevers purchased from Nanoworld with a nominal spring constant of 2.8 N/m and resonance frequencies in the range of 65–80 kHz were used for all AFM experiments.

Confocal Raman measurements were performed using the 532 nm excitation of a frequency-doubled neodymium-doped yttrium–aluminum–garnet (Nd:YAG) laser and a 20X objective lens with a numerical aperture of 0.40. A 488 nm diameter single-mode optical fiber was used to couple the laser beam into the microscope and a 50 μm diameter multi-mode optical fiber to couple the collected Raman scattering light to the spectrometer. The latter fiber acts both as a pinhole source for confocal microscopy and as an entrance slit for the spectrometer. A band-pass edge filter was used to eliminate the reflected laser line and (elastically) Rayleigh-scattered light. Each Raman spectrum was acquired for 500 miliseconds at a very low Nd:YAG laser power output of about 100 μW. The *WiTec Control 1.60* software was employed for such fast data acquisition.

3. RESULTS AND DISCUSSION

Since concentrations of neurotransmitters at physiological levels are between the nM and μM ranges, a key prerequisite for obtaining an intense Raman signature of a specific neurotransmitter is the use of efficient metal nanoparticles or nanostructures that provide a high level of electromagnetic field enhancement. By far, silver and gold have been the most biocompatible metals providing the greatest enhancement observed in SERS experiments [3,6–8,10]. Based on the previously mentioned importance of metal nanostructure characteristics in SERS performance, we first characterized the Ag NPs and Ag films by SEM and AFM. Images from these investigations are presented in Fig. 1 A–D. The images in Fig 1 A and B, which were acquired by SEM and AFM, respectively, reveal clustering and quite a large size distribution of the as-synthesized Ag NPs. Although this agglomeration impedes accurate determination of the relatively small sizes of the nanoparticles, it indicates a distribution of Ag NPs with dimensions from 5 nm to 20 nm. A closer look at these images confirms that the irregularly shaped large clusters are formed by coalesced Ag NPs with spherical shapes; isolated nanoparticles can also be seen in these images. The formation of the thin Ag film, which is presented in Fig. 1C and D at different magnifications, shows the expected aggregation of Ag NPs on the glass cover slip that occurred during the drop-casting process. Not only are Ag NPs' small sizes reconfirmed by these images, but additional information about the film's surface inhomogeneity is also provided. There are visible nano- and micro- indentations, which impart a surface roughness of ~50 nm to the film. Furthermore, since such idendations create randomly distributed "hot spots", they are beneficial for improving the quality of the SERS substrate and, consequently, for the desired enhancement of the Raman signal.

Raman spectroscopy can be used for both qualitative and relative quantitative analysis. Thus, an assessment of the intensities of characteristic Raman vibrational lines for the neurotransmitters under study as standards (purchased powders), on SERS substrates, and on glass cover slips are presented in Fig. 2 A–C. Concentrations of 10^{-5} M and 10^{-2} M have been used for measurements of neurotransmitters on SERS substrates and on glass cover slips, respectively. The corresponding structural

formulas of the compounds are shown in the insets. The low intensity of the Raman peaks for 10^{-2} M concentrations of the bioanalytes directly deposited on glass cover slips is clear evidence that neurotransmitters cannot be detected effectively at physiological levels (i.e., nM or μM levels) without the aid of SERS substrates; the Raman vibrations in these spectra are barely measurable. For these measurements, solutions of 10^{-2} M concentrations of neurotransmitters were drop-cast on the glass cover slips followed by vacuum drying to avoid their oxidation. Additional proof of the importance of the SERS substrates for detection of very low amounts of neurotransmitters is the fact that the Raman spectra of the standards (i.e., powders) and of the 10^{-2} M concentrations on glass cover slips were recorded with 100 times greater laser power than those acquired for the 10^{-5} M concentrations of neurotransmitters on SERS substrates. The overall Raman signals in the latter spectra, even for three orders of magnitude lower neurotransmitter concentrations and much lower laser power, are clearly much stronger than those corresponding to the analytes deposited only on glass cover slips. This observation, besides emphasizing that neurotransmitter detection can be easily achieved for much lower concentrations using SERS, also proves the quality of the substrates that were fabricated.

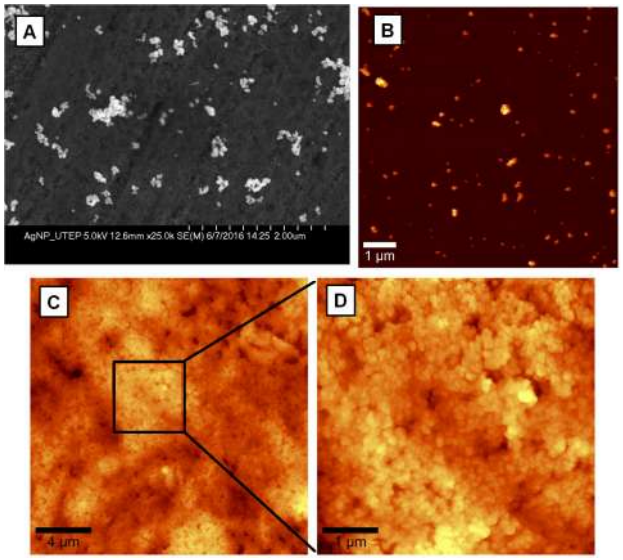

Figure 1: (A) SEM image of Ag NPs and **(B) – (D)** AFM images of Ag NPs, and of the thin film under different magnifications.

Some dominant bands observed in the Raman spectra of the standards completely disappear or shift in the SERS spectra of the neutrotransmitters, as previously reported in the literature [10,39–44]. For example, the dominant vibrational lines, of serotonin at 835 and 950 cm^{-1}, which correspond to the NH bending and the out-of-phase breathing modes of the indole ring, respectively [39,40], and of dopamine around 750 and 790 cm^{-1}, which are associated with the in-plane phenolic ring bending modes [43,44], are absent in the corresponding SERS spectra. Another example is the amine related Raman peak of adenosine at 858 cm^{-1} [41,42].

A plausible explanation of these vibrational band disappearances, especially in the case of dopamine and its derivative forms, is that at very low concentrations, positively charged amine groups interact more strongly with the negative Ag surface, via electrostatic attractive forces [39–44]. A dominant interaction with the formation of catechol–Ag bonding is expected at slightly higher concentrations within approximately the micromolar range [44]. At relatively high concentrations, such as 10^{-2} M, the density of molecules is high enough to result in a competition between molecule–molecule interactions and molecule–substrate interactions. Consequently, at such concentrations, interactions between positively charged amine groups and negatively charged cathecol groups produce corresponding bands in the Raman spectra. Their presence thus provides indirect confirmation of high neurotransmitter concentrations. On the other hand, at low concentrations, fewer molecules interact with each other and the molecule-Ag NP interactions become dominant.

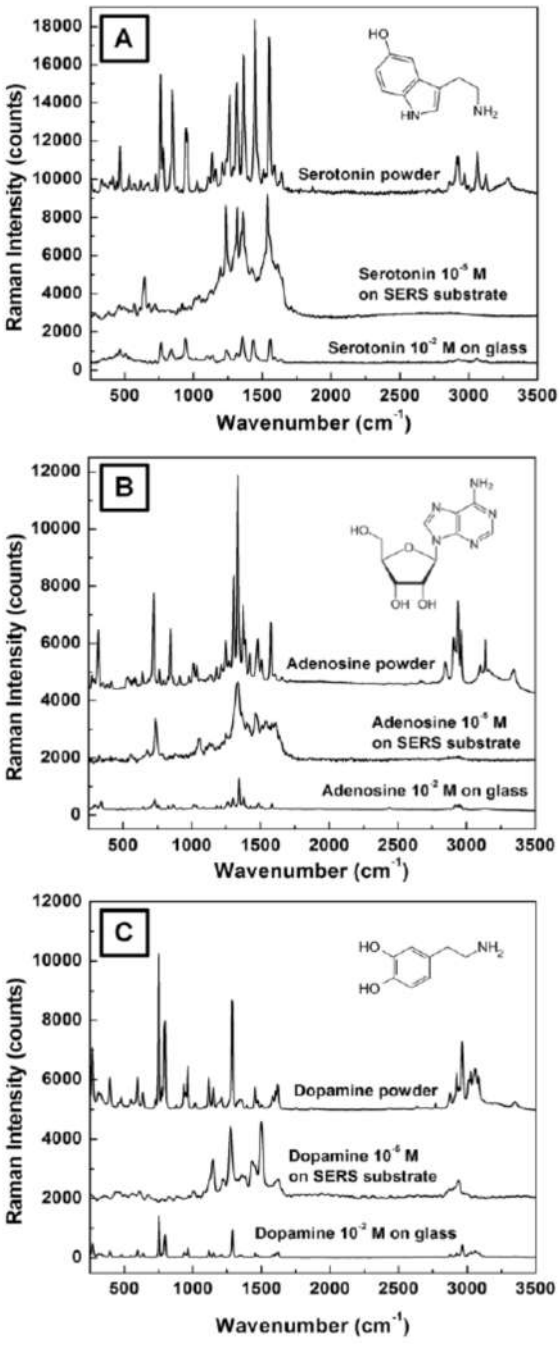

Figure 2. (A) – (C) Raman spectra of neurotransmitters recorded as standards (i.e., purchased powders), for 10^{-2} M concentrations deposited on glass cover slips, and for 10^{-5} M concentrations deposited on SERS substrates. The corresponding structural formulas of the compounds are presented in the insets. The spectra are vertically translated for easier visualization.

Due to the small ranges of the band shifts, they cannot be as easily depicted in the spectra of Fig. 2 A–C as the disappearance of the previously discussed vibrational lines. However, we still mentioned them in what follows. The Raman bands of serotonin at 762, 1260, 1309, 1363, 1450 cm^{-1}, and 1552 cm^{-1}, which are also assigned to in-phase breathing and stretching modes of the indole ring, shift towards lower wavenumbers at 645, 1235, 1301, 1347 cm^{-1}, 1425 cm^{-1}, and 1538 cm^{-1} in the SERS spectrum. This observation of downward shifts of serotonin Raman bands is consistent with previously reported results [39,40]. In the case of adenosine, the peak at 726 cm^{-1} that corresponds to the adenine ring breathing mode shifts to a higher frequency at 738 cm^{-1}, while the peak at 1342 cm^{-1} attributed to NH_2 vibration exhibits a downshift to 1335 cm^{-1} [41,42]. Dopamine shows a similar downshift behavior for the vibrational feature at 1288 cm^{-1}, which could be assigned to either the CH_2 bending mode of the protonated molecule [43] or to the carbon-oxygen stretching mode of the neutral molecule [44], and at 1598 cm^{-1}, which is attributed to the in-plane H–N–C bending mode that originates from protonated C–C bending vibrations. A shift to 1275 and 1500 cm^{-1} is observed for these vibrational lines, respectively. Again, a possible reason for these Raman band shifts is the formation of hydrogen bonds. The indole NH, considered as a proton donor, can interact strongly with negatively charged Ag ions on colloidal NP surfaces. It is also worth mentioning here that some Raman bands shift more than others due to their intrinsic Raman selectivity and preferential variation of SERS enhancement [39–44].

It is clear from Fig. 3 A–C that the Ag NP platform allows concentrations as low as 10^{-11} M to be detected, which is quite sensitive and even superior to some SERS substrates of more complex design [3,6–8,10,14,16,17]. The SERS spectra of serotonin, dopamine, and adenosine for concentrations ranging from 10^{-5} M to 10^{-11} M are presented in this figure. One intriguing phenomenon that is evident is a SERS enhancement of serotonin that is conspicuously greater than of adenosine or dopamine (as revealed in the figure by the number of Raman counts on the y-axes). Its origin is in the energy band-gaps between the highest occupied molecular orbitals and the lowest unoccupied molecular orbitals (HOMO-LUMO) of serotonin, adenosine, and dopamine. These band-gaps are 2.29 eV (532 nm) for serotonin [45], 3.35 eV (370 nm) for adenosine [46], and 3.2 eV (387 nm) for dopamine [47]. A resonant Raman effect with the laser excitation of 532 nm used for these measurements could thus contribute to the higher signal observed for serotonin, in comparison with those of adenosine and dopamine.

Another observation pertains to the selective enhancement of the Raman peaks with variation in concentration. For example, dominant peaks around 1167, 1235, 1347, and 1538 cm^{-1} are observed for serotonin, around 738, 1170, and 1335 cm^{-1} for adenosine, and around 1142, 1275, and 1500 cm^{-1} for dopamine. While their prevalence was discussed above, with exception of the feature around 1100 cm^{-1} that can be potentially attributed to NH indole–Ag interaction, it is worth pointing out here that an accurate discrimination between these neurotransmitters cannot be assessed without appropriate statistical analysis due to the close proximity of some of the bands to one another. While it would be possible to consider the use of graphene-metal substrates as an alternative [7,15], such studies lie outside the purpose of the current work.

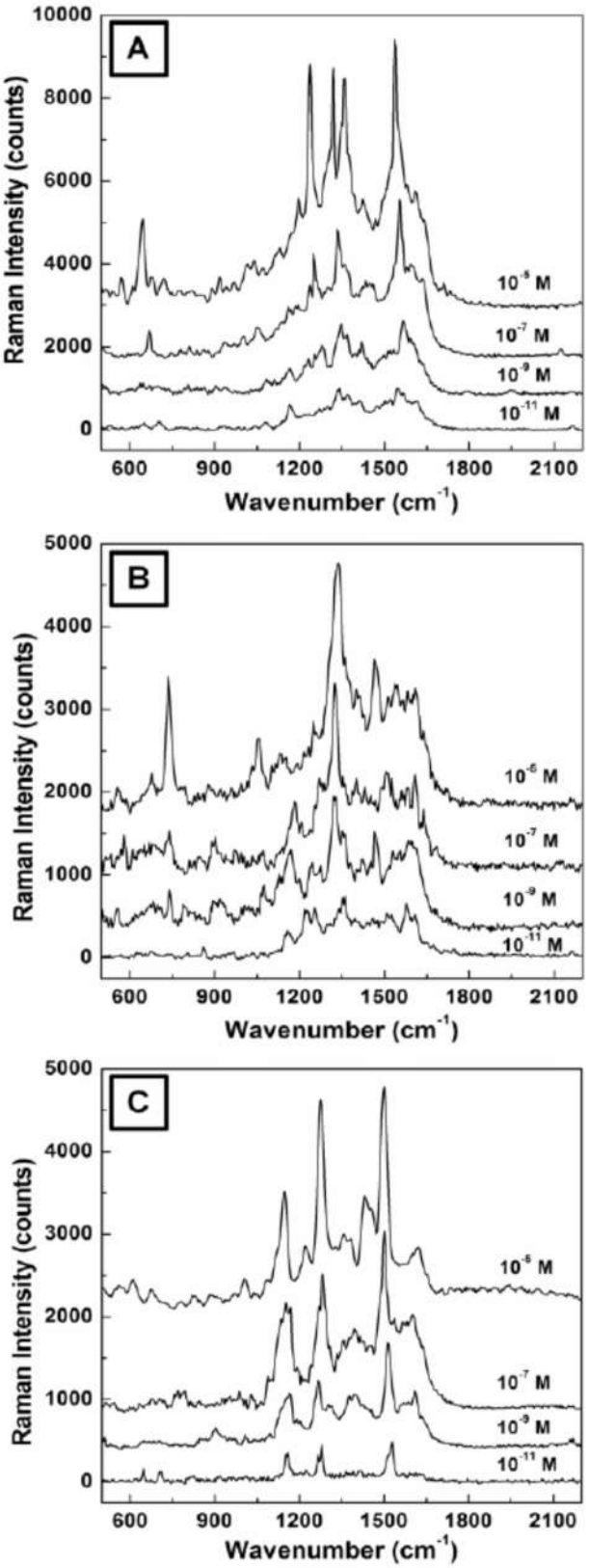

Figure 3. (A) – (C) SERS Raman spectra of serotonin, adenosine, and dopamine at different concentrations, as labeled.

4. CONCLUSIONS

In this study, fabrication of Ag NP SERS-active platforms enabled detection of serotonin, adenosine, and dopamine at concentrations as low as 10^{-11} molar. Besides demonstrating the potential value of this high sensitivity Raman recording of these very important analytes in the diagnosis of numerous neurological diseases, we observed variations in the intensities of characteristic Raman signatures that indicate changes in the molecular orientations of the neurotransmitters in the proximity of the silver surface, as well as potential chemical interactions. We also found that the intrinsically small Raman cross sections of neurotransmitter molecules and their densities close to the surface of Ag NPs play a significant role in preferential SERS enhancement. This study not only provides direct evidence that, using Raman spectroscopy, label-free detection of trace amounts of neurotransmitters is achievable, but it further advances knowledge of their interactions at the interface with metal nanoparticles.

5. REFERENCES

[1] Fleischmann M., Hendra P. J., McQuillan A. J. Raman Spectra of Pyridine Adsorbed at a Silver Electrode, *Chem. Phys. Lett.*, 26, 163–166, **1974**.

[2] Jeanmaire D. L., Van Duyne R. P. Surface Raman spectroelectrochemistryPart I. Heterocyclic, Aromatic, and Aliphatic Amines Adsorbed on the Anodized Silver Electrode, *J. Electroanal. Chem.*, 84, 1–20, **1977**.

[3] Kneipp J., Kneipp H., Kneipp K., SERS – a Single-Molecule and Nanoscale Tool for Bioanalytics. *Chem. Soc. Rev.*, 37, 1052–1060, **2008**.

[4] Gong X., Bao Y., Qiu C., Jiang, C., Individual Nanostructured Materials: Fabrication and Surface-Enhanced Raman Scattering, *Chem. Commun.*, 48, 7003–7018, **2012**.

[5] Vassalini I., Rotunno E., Lazzarini L., Alessandri I. "Stainless" Gold Nanorods: Preserving Shape, Optical Properties, and SERS Activity in Oxidative Environment, *ACS Appl. Mater. Interfaces*, 7, 18794–18802, **2015**.

[6] Jiang Z., Gao P. F., Yang L., Huang C. Z., Li Y. F. A Facile in Situ Synthesis of Silver Nanoparticles on the Surface of Metal-Organic Framework for Ultrasensitive SERS Detection of Dopamine, *Anal. Chem.*, 87, 24, 12177–12182, **2015**.

[7] Wang P., Xia M., Liang O., Sun K., Cipriano A. F., Schroeder T., Liu H., Xie Y.H. Label-Free SERS Selective Detection of Dopamine and Serotonin Using Graphene-Au Nanopyramid Heterostructure, *Anal. Chem.*, 87, 10255–10261, **2015**.

[8] Qian X.-M., Nie S. M., Single-Molecule and Single-Nanoparticle SERS: From Fundamental Mechanisms to Biomedical Applications, *Chem. Soc. Rev.*, 37, 912–920, **2008**.

[9] Manciu F. S., Lee K. H., Durrer W. G., Bennet K. E., Detection and Monitoring of Neurotransmitters--a Spectroscopic Analysis. *Neuromodulation*, 16, 192–199, **2013**.

[10] Qin L., Li X., Kang S.-Z., Mu J., Gold Nanoparticles Conjugated Dopamine as Sensing Platform for SERS Detection, *Colloids Surfaces B Biointerfaces*, 126, 210–216, **2015**.

[11] Halvorson R. A., Vikesland P. J. Surface-Enhanced Raman Spectroscopy (SERS) for Environmental Analyses, *Environ. Sci. Tech.*, 44, 7749–7755, **2010**.

[12] Dasary S. S. R., Singh A. K., Senapati D., Yu H., Ray P. C. Gold Nanoparticle Based Label-Free SERS Probe for Ultrasensitive and Selective Detection of Trinitrotoluene, *J. Am. Chem. Soc.*, 131, 13806–13812, **2009.**

[13] Golightly R. S., Doering W. E., Natan M. J., Surface-Enhanced Raman Spectroscopy and Homeland Security: A Perfect Match? *ACS Nano*, 3, 2859–2869, **2009**.

[14] Dutta S., Ray C., Sarkar S., Pradhan M., Negishi Y., Pal T., Silver Nanoparticle Decorated Reduced Graphene Oxide (rGO) Nanosheet: A Platform for SERS Based Low-Level Detection of Uranyl Ion, *ACS Appl. Mater. Interfaces*, 5, 8724–8732, **2013**.

[15] Qiu C., Bennet K. E., Khan T., Ciubuc J. D., Manciu F. S. Raman and Conductivity Analysis of Graphene for Biomedical Applications. *Materials*, 9, 897–908, **2016**.

[16] Sinha G., Depero L. E., Alessandri I., Recyclable SERS Substrates Based on Au-Coated ZnO Nanorods. *ACS Appl. Mater. Interfaces*, 3, 2557–2563, **2011**.

[17] Wang Y., Zhao X., Chen L., Chen S., Wei M., Gao M., Zhao Y., Wang C., Qu X., Zhang Y., *et al.,* Ordered Nanocap Array Composed of SiO2-Isolated Ag Islands as SERS Platform, *Langmuir, 30*, 15285–15291, **2014**.

[18] Ansar S. M., Li X., Zou S., Zhang D. Quantitative Comparison of Raman Activities, SERS Activities, and SERS Enhancement Factors of Organothiols: Implication to Chemical Enhancement, *J. Phys. Chem. Lett.*, 3, 560–565, **2012**.

[19] Qiu C., Zhang L., Wang H., Jiang C. Surface-Enhanced Raman Scattering on Hierarchical Porous Cuprous Oxide Nanostructures in Nanoshell and Thin-Film Geometries, *J. Phys. Chem. Lett.*, 3, 651–657, **2012**.

[20] Meyer S. A., Le Ru E.C ., Etchegoin P. G. Combining Surface Plasmon Resonance (SPR) Spectroscopy with Surface-Enhanced Raman Scattering (SERS), *Anal. Chem.*, 83, 2337–2344, **2011**.

[21] Jeon T. Y., Park S. G., Lee S. Y., Jeon H. C., Yang S. M., Shape Control of Ag Nanostructures for Practical SERS Substrates. *ACS Appl. Mater. Interfaces*, 5, 243–248, **2013**.

[22] Teodorescu C. M., Image molecular dipoles in surface enhanced Raman scattering, *Phys. Chem. Chem. Phys.*, 17, 21302–21314, **2015**.

[23] de la Fuente-Fernández R., Ruth T. J., Sossi V., Schulzer M., Calne D. B., Stoessl A. J., Expectation and Dopamine Release: Mechanism of the Placebo Effect in Parkinson's Disease, *Science*, 293, 1164–1166, **2001**.

[24] Fox S. H., Chuang R., Brotchie J. M., Serotonin and Parkinson's Disease: On Movement, Mood, and Madness, *Movem. Disord.*, 24, 1255–1266, **2009**.

[25] Cechova S., Venton B. J. Transient Adenosine Efflux in the Rat Caudate- Putamen, *J. Neurochem.*, 105, 1253–1263, **2008**.

[26] Njagi J., Chernov M. M., Leiter J. C, Andreescu, S. Amperometric Detection of Dopamine in Vivo with an Enzyme Based Carbon Fiber Microbiosensor, *Anal. Chem.*, 82, 989–996, **2010**.

[27] Phillips T. M., Measurement of bioactive neuropeptides using a chromatographic imunosensor cartridge, *Biomed. Chromatogr.*, 10, 331–336, **1996**.

[28] Stewart A. J., Hendry J., Dennany L., Whole Blood Electrochemiluminescent Detection of Dopamine, *Anal. Chem.*, 87, 11847–11853, **2015**.

[29] Zhang L., Cheng Y., Lei J., Liu Y. Hao Q., Ju H., Stepwise Chemical Reaction Strategy for Highly Sensitive Electrochemiluminescent Detection of Dopamine., *Anal. Chem.*, 85, 8001–8007, **2013**.

[30] Cui R., Gu Y.-P., Bao L., Zhao J.-Y., Qi B.-P., Zhang Z.-L., Xie Z.-X., Pang D.-W. Near-Infrared Electrogenerated Chemiluminescence of Ultrasmall Ag2Se Quantum Dots for the Detection of Dopamine., *Anal. Chem.*, 84, 8932–8935, **2012**.

[31] Zeltser L. M., Seeley R. J., Tschop M. H., Synaptic plasticity in neuronal circuits regulating energy balance, *Nature Neurosci.*, 15, 10, 1336–1342, **2012**.

[32] Meister B., Neurotransmitters in key neurons of the hypothalamus that regulate feeding behavior and body weight. *Physiol. Behav.*, 92, 1-2, 263–271, **2007**.

[33] Willis D., Li K. W., Zheng J. Q., Chang J. H., Smit A., Kelly T., Merianda T. T., Sylvester J., van Minnen .J, Twiss J. L. Differential Transport and Local Translation of Cytoskeletal, Injury-Response, and Neurodegeneration Protein mRNAs in Axons. *J. Neurosci.*, 25, 778–791, **2005**.

[34] Huh W. K., Falvo J. V., Gerke L. C., Carroll A. S., Howson R. W., Weissman J. S., O'Shea E. K. Global analysis of protein localization in budding yeast, *Nature*, 425, 686–691, **2003**.

[35] Kondo D. G., Hellem T. L., Sung Y.-H., Kim N., Jeong E. K., DelMastro K. K., Shi X., Renshaw P. F. Review: Magnetic Resonance Spectroscopy Studies of Pediatric Major Depressive Disorder, *Depression Res. Treat.*, 2011, 1–13, **2011**.

[36] Shon Y. M., Chang S. Y., Tye S. J., Kimble C. J., Bennet K. E., Blaha C. D., Lee K. H., Co-monitoring of adenosine and dopamine using the Wireless Instantaneous Neurotransmitter Concentration System: proof of principle, *J. Neurosurg.*, 112, 539–548, **2010**.

[37] Bennet K. E., Tomshine J. R., Min H.-K., Manciu F. S., Marsh M. P., Paek S. B., Settell M. L., Nicolai E. N., Blaha C. D., Kouzani A. Z., Chang S.-Y., Lee K. H., A Diamond-Based Electrode for Detection of Neurochemicals in the Human Brain, *Front. Human Neurosci.*, 10, 102, 1–12, **2016**.

[38] Wan Y., Guo Z., Jiang X., Fang K., Lu X., Zhang Y., Gu N., Quasi-Spherical Silver Nanoparticles: Aqueous Synthesis and Size Control by the Seed-Mediated Lee-Meisel Method, *J. Colloid Interface Sci.*, 394, 263–268, **2013**.

[39] Song P., Guo X., Pan Y., Wen Y., Zhang Z., Yang H., SERS and *in situ* SERS spectroelectrochemical investigations of serotonin monolayers at a silver electrode, *J. Electroanal. Chem.*, 688, 384–391, **2013**.

[40] Tu Q., Eisen J., Chang C., Surface-enhanced Raman spectroscopy study of indolic molecules adsorbed on gold calloids, *J. Biomed. Opt. Lett.*, 15(2), 020512-1–3, **2010**.

[41] Kundu J., Neumann O., Janesko B. G., Zhang D., Lal S., Barhoumi A., Scuseria G. E., Halas N. J., Adenine– and Adenosine Monophosphate (AMP) – Gold Binding Interactions Studied by Surface-Enhanced Raman and Infrared Spectroscopies, *J. Phys. Chem. C*, 113 14390–14397, **2009**.

[42] Lee S. A., Anderson A., Smith W., Griffey R. H. Mohan V. Temperature- dependent Raman and infrared spectra of nucleosides. Part I – adenosine, *J. Raman Spectrosc.*, 31, 891–896, **2000**.

[43] Pande S., Jana S., Sinha A. K., Sarkar S., Basu M., Pradhan M., Pal A., Chowdhury J., Pal T. Dopamine Molecules on A_{ucore}–Ag_{shell} Bimetallic Nanocolloids: Fourier Transform Infrared, Raman, and Surface-Enhanced Raman Spectroscopy Study Aided by Density Functional Theory, *J. Phys. Chem. C*, 113, 6989–7002, **2009**.

[44] Palanisamy S., Yan L., Zhang X., He T., Surface enhanced Raman scattering - active worm-like Ag clusters for sensitive and selective detection of dopamine. *Anal. Methods*, 7, 3438–3447, **2015**.

[45] Weinberg J., Lerner D. A., Balaceanu-Stolnici C., Theoretical Study of DHEAS: the Electronic Properties of a Complex between DHEAS and Serotonin by Comparative Calculations HF and DFT, *Revue Roumaine de Chimie*; 52, 8–9, 759–764, **2007**.

[46] Murugan N., Wihelm Hugosson H., Solvent Dependence of Conformational Distribution, Molecula Geometry, and Electronic Structure of Adenosine, *J. Phys. Chem.*, 113, 1012-1021, **2009**.

[47] Mohammad-Shiri H., Ghaemi M., Riahi S., Akbari-Sehat A., Computational and Electrochemical Studies on the Redox Reaction of Dopamine in Aqueous Solution, *Int. J. Electrochem. Sci.,* 6, 317 – 336, **2011**.

6. ACKNOWLEDGEMENTS

This work was supported by the NIH NIMHHD 2G12MD007592 award and by a research agreement between the University of Texas at El Paso and the Mayo Clinic.